Application of a data-assimilative regional ocean modeling system for assessing California Current System ocean conditions, krill, and juvenile rockfish interannual variability

Isaac D. Schroeder[1,2], Jarrod A. Santora[3,4], Andrew M. Moore[5], Christopher A. Edwards[5], Jerome Fiechter[5], Elliott L. Hazen[2], Steven J. Bograd[2], John C. Field[4], and Brian K. Wells[4]

[1]Division of Physical and Biological Sciences, University of California at Santa Cruz, Santa Cruz, California, USA, [2]Environmental Research Division, Southwest Fisheries Science Center, NOAA Fisheries, Pacific Grove, California, USA, [3]Center for Stock Assessment Research, University of California at Santa Cruz, Santa Cruz, California, USA, [4]Fisheries Ecology Division, Southwest Fisheries Science Center, NOAA Fisheries, Santa Cruz, California, USA, [5]Department of Ocean Sciences, University of California at Santa Cruz, Santa Cruz, California, USA

Abstract To be robust and informative, marine ecosystem models and assessments require parameterized biophysical relationships that rely on realistic water column characteristics at appropriate spatial and temporal scales. We examine how hydrographic properties off California from 1990 through 2010 during late winter and spring correspond to krill and juvenile rockfish (*Sebastes* spp.) abundances. We evaluated coherence among temperature, salinity, depth of 26.0 potential density isopycnal, and stratification strength at regionally and monthly time scales derived from shipboard and mooring observations, and a data-assimilative Regional Ocean Model System reanalysis. The reanalysis captures spatiotemporal physical variability of coastal ocean conditions in winter and spring months and elucidates mechanisms connecting the spatial and temporal upwelling and transport dynamics on observed krill and rockfish abundances in spring. This provides evidence for a mechanistic connection between the phenology of upwelling in the California Current System and seasonal development of the shelf ecosystem.

1. Introduction

Krill are important prey species of upper trophic level predators in eastern boundary upwelling ecosystems, such as the California Current System. Interannual variability of krill abundance is greatest within shelf waters [*Santora et al.*, 2014] and corresponds to the feeding activity and early survival of juvenile Pacific salmon (*Oncorhynchus* spp.) [*Wells et al.*, 2012], the demographic characteristics of seabird colonies [*Ainley et al.*, 1995], and the distribution of marine mammals [*Croll et al.*, 2005]. Juvenile rockfish (*Sebastes* spp.) feed on krill during spring and summer following winter parturition (larval release of rockfish) [*Reilly et al.*, 1992], are prey for salmon [*Thayer et al.*, 2014], and are critical to the reproductive success of piscivorous seabirds [*Wells et al.*, 2008; *Field et al.*, 2010]. Quantifying the links between spatiotemporal dynamics of ocean conditions and variability in krill and rockfish abundances on the shelf can provide insights into the mechanisms leading to a productive California Current System.

In the Gulf of the Farallones, a highly productive shelf region off central California, krill and juvenile rockfish abundances during the spring are greatest during years of strong upwelling and cool surface temperatures, and are low during years of weak upwelling and warm surface temperatures [*Santora et al.*, 2014]. The evolution of upwelling conditions in late winter is also linked to biological production on the shelf during the spring/summer upwelling season [*Bograd et al.*, 2009; *Schroeder et al.*, 2009, 2013]. Although *Santora et al.* [2013] applied an ocean-ecosystem model to evaluate observed and modeled krill abundance, the ocean conditions that promote development of a productive shelf community have not been examined at all scales relevant to that community [*Santora et al.*, 2012].

The Regional Ocean Modeling System (ROMS) framework offers a widely used platform for realistic ocean circulation modeling [*Shchepetkin and McWilliams*, 2005]. Advanced data assimilation capability constrains model solutions with observations, producing an estimate of the ocean state that is closer to nature than unconstrained solutions [*Moore et al.*, 2011]. By incorporating spatially and temporally explicit oceanographic
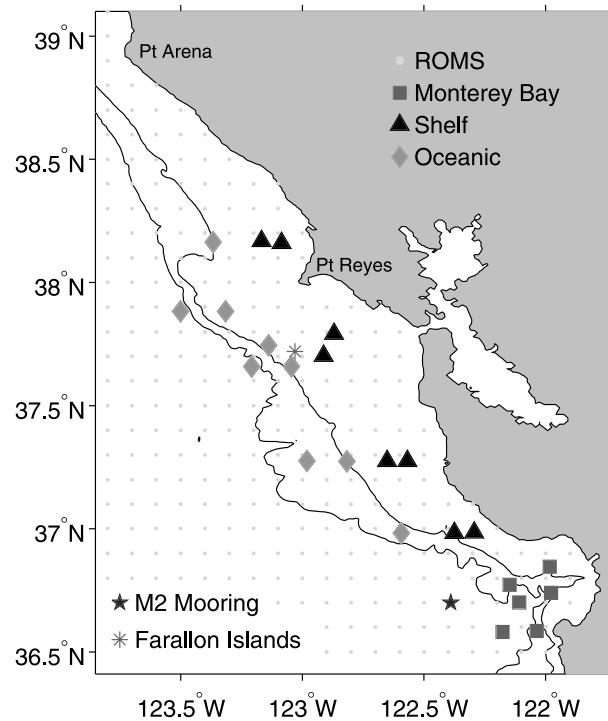
Figure 1. Map of the area sampled by the RREAS during May–June. Hydrographic profiles and trawls are conducted at the stations, and the stations are divided into three distinct ecological regions: Monterey Bay, shelf, and oceanic.

observations (e.g., satellite, shipboard, and mooring), improved data-assimilative state estimates offer a promising approach to quantify the contributions of environmental factors to biological variability in marine ecosystems [*Fiechter et al.*, 2011].

Here, we use a ROMS reanalysis to elucidate the spatiotemporal water column characteristics that correspond to variability of krill and rockfish abundances during spring and summer. Our first objective evaluates the capacity of the reanalysis to represent direct observations of water column properties at spatial (~10–100 km) and temporal (monthly) scales previously determined to be relevant to the shelf community [*Santora et al.*, 2012, 2014; *Schroeder et al.*, 2013]. Therefore, variables derived from ROMS output were selected based on the results of *Santora et al.* [2014], wherein subsurface temperature and salinity averaged between 20 and 40 m, depth of $\sigma_\theta = 26.0$ isopycnal, and density stratification strength between 0 and 100 m are related to krill distribution and abundance on the shelf. Twenty-four years of hydrographic observations collected from shipboard surveys off central California during May–June provide independent (unassimilated) information from ROMS output for spatial and interannual comparisons. Simulated seasonal variability of hydrographic conditions is evaluated against measurements from the M2 mooring in Monterey Bay, which provides hydrographic data throughout the year. For our second objective, we derive statistical relationships between simulated environmental conditions in winter and spring and observed krill and rockfish abundances on the shelf in May–June.

We hypothesize that regional upwelling characteristics preceding spring influence krill and rockfish abundances off coastal central California. Conceptually, upwelling intensity in late winter influences abundance of krill on the shelf through associated transport dynamics [*Dorman et al.*, 2005] and initial nutrient introduction [*Croll et al.*, 2005]. During spring, krill are maintained on the shelf by reduced advection [*Graham and Largier*, 1997] and continued nutrient introduction [*Steger et al.*, 2000; *Largier et al.*, 2006]. Regional upwelling and transport dynamics following winter parturition of larvae at the shelf break determine rockfish abundance on the shelf in spring [*Ralston et al.*, 2013] and, once there, they subsist largely on krill [*Reilly et al.*, 1992].

2. Data and Methods

2.1. In Situ Hydrographic and Biological Data

The National Marine Fisheries Service conducts an annual Rockfish Recruitment and Ecosystem Assessment Survey (RREAS) to sample micronekton off central California (approximately 36.5°N to 38.2°N and ~65 km offshore; Figure 1). The RREAS consistently samples stations during May and June, with each station sampled 1 to 3 times per survey. At each station, a conductivity-temperature-depth (CTD) cast and a midwater trawl were used to collect physical and biological data. For a complete account of the sampling protocols of the RREAS see *Ralston et al.* [2013]. For our analysis we use stations that have at least 20 years of hydrographic data for the time period 1987 to 2010. Krill (all species) and juvenile rockfish (ten most abundant species) were enumerated from the trawl samples and time series of geometric means of catch-per-unit-effort (CPUE) were calculated for each station (data was available 1990–2010, Figure 1). During May–June, pelagic juvenile rockfish

Table 1. Normalized Standard Deviations (σ_m/σ_o), Pearson Correlations (r), Root Mean Squared Errors (RMS), and Bias (b) Between May–June Rockfish Recruitment and Ecosystem Assessment Survey (RREAS) and Data Assimilative Regional Ocean Modeling System (ROMS) Time Series for Three Regions in Central California[a]

	Region	σ_m/σ_o	r	RMS	b
Temperature	MB	0.92	0.68	0.51	**0.36**
	Shelf	1.28	0.63	0.62	**0.64**
	Oceanic	1.20	0.66	0.62	0.26
Salinity	MB	0.89	0.89	0.08	−0.03
	Shelf	1.09	0.86	0.09	**−0.11**
	Oceanic	0.96	0.88	0.10	0.01
$\sigma_\theta = 26.0$ depth	MB	0.89	0.63	17.58	**11.20**
	Shelf	1.60	0.60	19.35	**18.26**
	Oceanic	1.61	0.65	21.38	**15.43**
Stratification	MB	1.71	0.82	906.76	**1775.67**
	Shelf	0.75	0.84	843.89	**−2049.73**
	Oceanic	0.60	0.91	762.94	**−1927.42**

[a]All correlations are significant at $p < 0.01$. The units for columns RMS and b for temperature, depth, and stratification are °C, m, and J m^{-2}, respectively. Bold font marks a significant bias between the observational and model mean. The lengths of the Rockfish Recruitment and Ecosystem Assessment Survey (RREAS) and Regional Ocean Modeling System (ROMS) interannual time series are 24 years, 1987–2010.

encountered in the survey are approximately 3 to 4 months old and not yet associated with bottom habitat. We constructed krill and rockfish interannual time series by averaging the May and June sample CPUEs for shelf stations from the north of Monterey Bay to San Francisco Bay (Figure 1).

2.2. Mooring Data

The M2 mooring is located offshore of Monterey Bay (36.70°N 122.39°W; Figure 1) in water 1800 m deep; it is maintained by the Monterey Bay Aquarium Research Institute (MBARI). The MBARI mooring data have daily temperature and salinity data from July 1998 to the present for the following depths: 1, 10, 20, 40, 60, 80, 100, 150, 200, 250, and 300 m (http://www.mbari.org/oasis/).

2.3. The ROMS Reanalysis

The ocean modeling group at the University of California, Santa Cruz has completed an historical (1980–2010) reanalysis of the California Current System using the ROMS 4-Dimensional variational data assimilation system [*Moore et al.*, 2011; http://oceanmodeling.pmc.ucsc.edu/]. The model assimilated available satellite sea surface temperature, altimetry data, and in situ hydrographic data. The in situ hydrographic data were taken from the quality controlled EN3 data set (v2a) maintained by the UK Met Office [*Ingleby and Huddleston*, 2007]. The model's spatial resolution is 1/10° in the horizontal and 42 terrain-following σ-levels in the vertical, and run with a 15 min time step. The model configuration is described in detail by *Veneziani et al.* [2009]. Importantly, neither the RREAS nor M2 mooring data were used in the ROMS assimilation so model output is independent of the observational data. Six-hour snapshots of the model output were averaged to 1 day intervals for the reanalysis evaluation.

2.4. Reanalysis Evaluation

The closest model grid point to RREAS stations and M2 mooring were used for the evaluation (Figure 1). Daily values from M2 and dates of CTD collections were matched to daily averaged ROMS reanalysis output. Time series, including monthly averaged mooring data and spring averages for RREAS data, were linked to equivalent time series from the ROMS reanalysis. We examined mean temperature and salinity between 20 and 40 m, depth of the 26.0 potential density isopycnal, and stratification between 0 and 100 m for RREAS stations, the M2 mooring, and the corresponding ROMS grid points. The 26.0 isopycnal depth represents the base of the pycnocline, an area of high nutrients [*Palacios et al.*, 2013] that shoals during upwelling [*Lynn et al.*, 2003]. At the location of the M2 mooring the $\sigma_\theta = 26.0$ isopycnal depth is on average located at ~100 m and ranges from 160 m to the surface; these isopycnal displacements are due to a combination of upwelling, circulation, and alongshore transport features [*Collins et al.*, 2003]. Therefore, variability in the 26.0 isopycnal depth corresponds to upwelling intensity and associated nutrient introduction and transport dynamics. Our measure of stratification is the integrated potential energy (J m^{-2}) from the surface to 100 m relative to
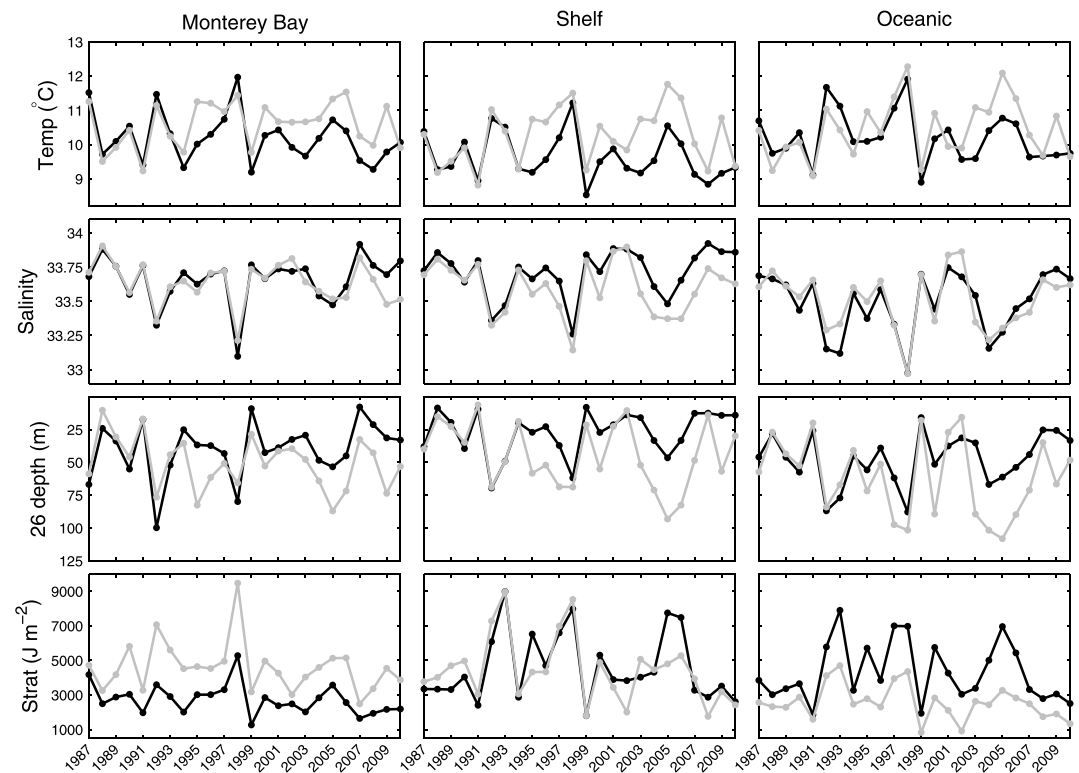
Figure 2. Time series comparing the RREAS (black) with the assimilative ROMS (gray) for the three regions (Monterey Bay, shelf, and oceanic) and four environmental indices (temperature, salinity, stratification, and 26.0 isopycnal depth). Each time series consist of an average May–June value for the years 1987 to 2010.

the mean density over the 100 m interval [*Ladd and Stabeno*, 2012]. To reduce spatial variability in the RREAS, stations were averaged in three regions identified by *Santora et al.* [2012, 2014] to be physically and ecologically similar in May–June: Monterey Bay, shelf, and oceanic (Figure 1). Monthly means of the four variables were constructed for the daily M2 mooring data for the years 1998 to 2010.

To evaluate coherence among observational (RREAS and M2) and model time series, we calculated the Pearson correlation (r), root mean square error (RMS), standard deviation of the model output (σ_m) relative to the observational (σ_o), and bias ($b = \bar{m} - \bar{o}$, where $\bar{m}$ and $\bar{o}$ are the means of the model and observational time series, respectively). A paired *t* test was used to determine if there was significant bias between model output and observations. The results from the evaluations between ROMS and M2 mooring data are displayed as Taylor diagrams [*Taylor*, 2001]. To quantify relationships among krill and rockfish abundances and ocean conditions, we created spatial correlation maps between krill and rockfish interannual time series ($n = 21$), and monthly means of the four environmental indices derived from ROMS for grid locations between 36.4°N and 39.4°N and 126°W to 122°W for the months January through June.

3. Results

3.1. Coherence Between Shipboard Observations and the ROMS Reanalysis

Across three ecological regions, RREAS and model data display similar interannual variability in temperature, depth of the 26.0 isopycnal, salinity, and stratification (Table 1 and Figure 2, for station-specific statistics see Figure S.1), and correlations between ROMS output and observed data were significantly positive for all four variables. However, the reanalysis exhibited significant biases relative to observations for all four variables across the three regions (Table 1, Figure 2, and Figure S.1).

3.2. Monthly Coherence Between Mooring Observations and the ROMS Reanalysis

Monthly temperature, salinity, stratification, and 26.0 isopycnal depth derived from ROMS output were coherent with M2 mooring data (Figure 3 and Figure S.2). Correlations between mooring observations and
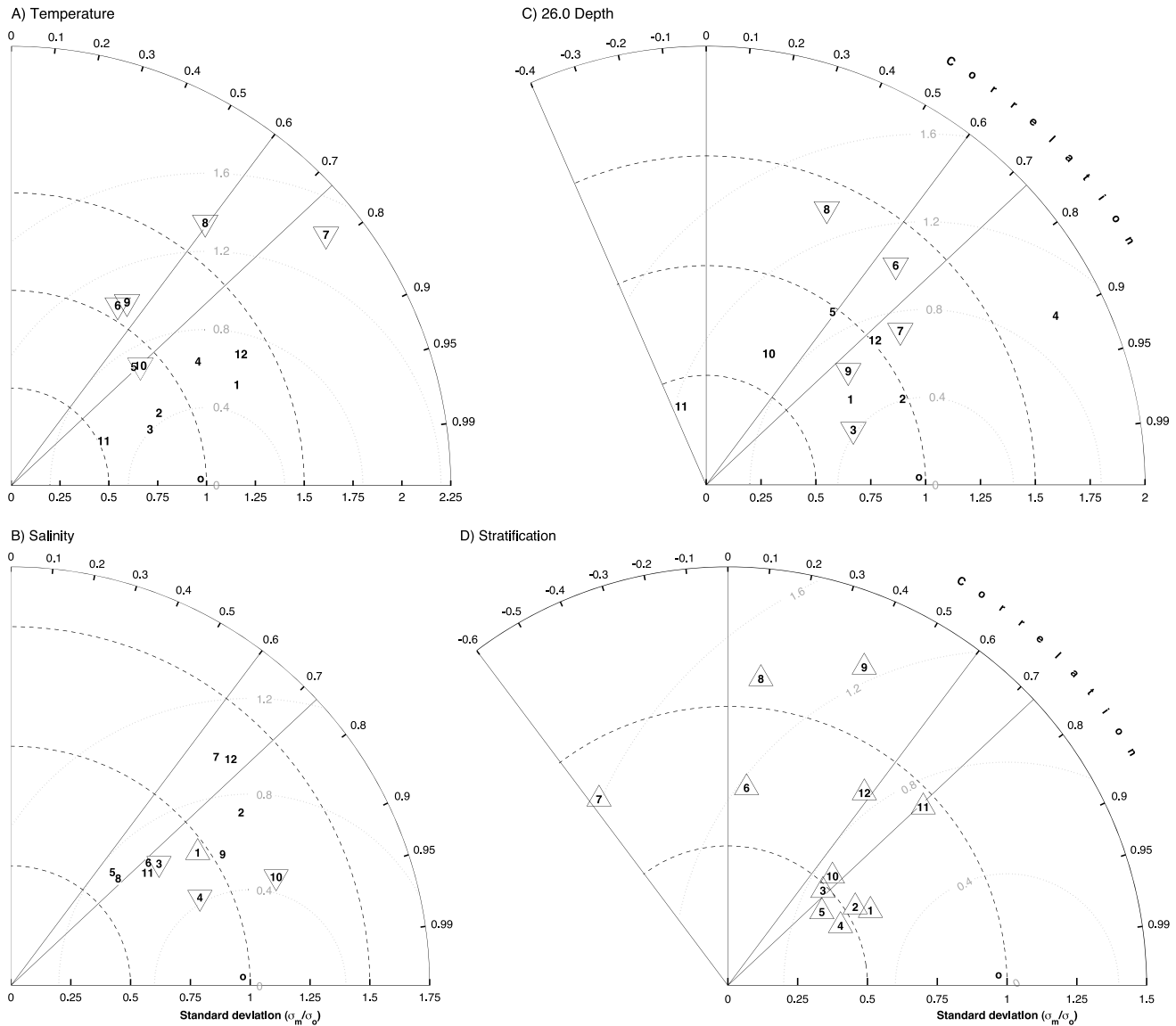
Figure 3. Taylor diagrams for the comparison of monthly (January–December symbols 1–12) time series of M2 mooring data with ROMS output for temperature, salinity, 26.0 isopycnal depth, and stratification. The radial coordinate of the Taylor diagram is the normalized standard deviation (σ_m/σ_o), the angular coordinate is the Pearson correlation (r), and the RMS error is proportional to the distance from the observational (letter o) to the symbols (1–12). Axes of the RMS error are displayed as concentric circles about the letter o label. Also, in the figure a triangle pointing down denotes a positive bias, and a triangle pointing up indicates a negative bias between the observational and model mean. Two angular correlation lines are drawn in black: 0.60 ($p = 0.05$) and 0.73 ($p = 0.01$).

reanalysis output were highest for winter and spring months (January through June; Figure 3 and Figure S.2). There were a number of significant and inconsistent biases between the ROMS output and independent observations for temperature, salinity, and 26.0 isopycnal depth. ROMS output consistently underestimated observed stratification.

3.3. Spatiotemporal Coherence Between Krill and Rockfish and the Reanalysis

We performed a temporally lagged spatial correlation analysis between observed May–June average krill and rockfish abundances with 26.0 isopycnal depth from ROMS output over the individual months of January through June (Figure 4). We emphasize the results from isopycnal depth because it relates to upwelling [*Collins et al.*, 2003], the associated shoaling of nutrients, and the likely transport of those nutrients [*Santora et al.*, 2012]. As well, although unexamined directly, isopycnal depth corresponds with horizontal advection
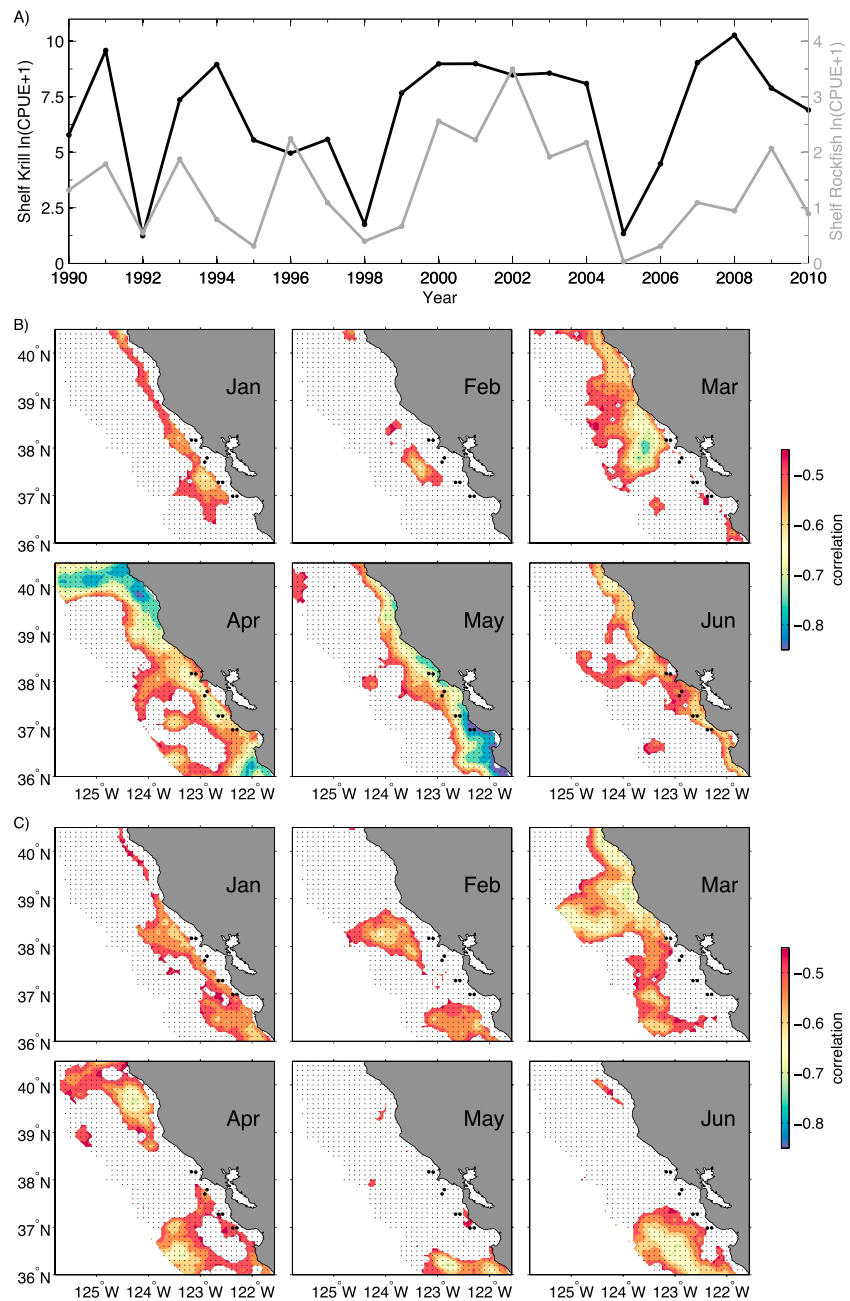
Figure 4. (a) Interannual time series log-transformed abundance of krill (black) and juvenile rockfish (gray), and spatial correlation maps derived from Spearman's rank correlations between (b) krill and (c) juvenile rockfish time series and 26.0 isopycnal depth time series derived from a data assimilative ROMS model. Krill and juvenile rockfish data were collected during May and June in central California at stations on the shelf (black circles). The time series of 26.0 isopycnal depth from each location marked by a gray dot are monthly means for January through June. Only correlations with $p < 0.05$ are shown; areas in white represent non-significant correlations.

significant enough to transport krill [*Dorman et al.*, 2011] and juvenile rockfish [*Petersen et al.*, 2010]. All significant ($p < 0.05$) correlations were negative, implying that a shallower 26.0 isopycnal depth corresponds to greater krill and rockfish abundances.

Areas of high correlations are apparent adjacent to the shelf during January and February, suggesting that late-winter upwelling conditions may precondition the system for higher springtime abundances of krill and rockfish. The strongest correlations between krill abundance and oceanographic conditions were found for the

months of March through June (Figure 4). During March, strongest correlations with krill correspond to an area offshore of Pt Reyes, while in April they are located near Pt Arena (Figure 4). By May and June, krill abundance was highly correlated to isopycnal depth throughout the central California domain, most significantly nearshore (Figure 4). The extent and magnitude of the significant correlations between rockfish and isopycnal depth highlight the importance of ocean conditions in areas outside the RREAS survey region, with significant correlations located near Pt Arena and offshore from the shelf break in the months of January through April. Compared to January through April, significant correlations between rockfish and isopycnal depth declined markedly during May and June (Figure 4).

The remaining three simulated variables (temperature, salinity, and stratification) were also examined for this analysis; however, for brevity those results are displayed in the supplement (Figure S.3 and Figure S.4). In short, krill abundance correlations to temperature, salinity, and stratification provided spatiotemporal patterns consistent with those associated with the 26.0 isopycnal depth variations (Figure S.3). Juvenile rockfish abundance correlated to salinity in March across much of the region and only south of the Gulf of the Farallones April through June (Figure S.4).

4. Discussion

We evaluated a data-assimilative ROMS reanalysis using shipboard survey and mooring data across three ecological regions of the central California coast and throughout the year. We found that the model captured the interannual variability of hydrographic conditions within the three regions during May–June (Table 1, Figure 2, and Figure S.1). The temporal evaluation revealed that the ROMS reanalysis was most consistent with observations from January to June (Figure 3). Importantly, we demonstrate significant biases in the ROMS output. Therefore, we have restricted our analysis to a correlative approach. Currently, we have no explanation for the seasonally varying biases that develop with respect to subsurface observations.

Regional upwelling characteristics leading up to spring influence krill and rockfish abundances off coastal central California. Krill and rockfish abundances are correlated to isopycnal depth occurring at least 4 months prior (Figure 4, Figure S.3, and Figure S.4), suggesting spring and summer populations of krill and rockfish on the shelf are partly determined by conditions in the winter [*Schroeder et al.*, 2009; *Ralston et al.*, 2013]. Relevant to krill abundance, the correlations with coastal isopycnal depth are consistent with improved krill production as a result of late-winter and spring coastal upwelling and southward transport of nutrients to the Gulf of the Farallones [*Steger et al.*, 2000; *Croll et al.*, 2005; *Dorman et al.*, 2005], which has the potential to affect krill spawning dynamics and increase egg densities [*Feinberg and Peterson*, 2003]. However, the confounded effects of upwelling and transport cannot be parsed with only the isopycnal depth value. It is also likely that winter transport of krill is an important factor for maintaining a resident krill population [*Dorman et al.*, 2011]. Juvenile rockfish abundance correlates to offshore isopycnal depth during the time of parturition at the shelf break, and the correlations weaken and are more southerly as spring approaches (Figure 4). The temporally lagged correlations between juvenile rockfish abundance and isopycnal depth may represent transport to the shelf [*Chelton et al.*, 1982; *Graham and Largier*, 1997] and/or better feeding conditions immediately following parturition [*Houde*, 2008]. Once present on the shelf in spring, juvenile rockfish abundance is not correlated to the environmental indices from the ROMS model but is spatially correlated with krill abundance [*Santora et al.*, 2014]. The results are consistent with our conceptual model and *Wells et al.* [2008], wherein, it was demonstrated that regionally averaged offshore windsheer during spring relates to rockfish productivity directly, while coastal upwelling relates to rockfish productivity indirectly through its influence on krill abundance.

A number of species in and around the Gulf of the Farallones have life histories related to winter conditions that lead them to rely on krill being present on the shelf in May as a prey resource. For instance, egg laying dates for some planktivorous seabird species (e.g., Cassin's Auklet *Ptychoramphus aleuticus*) are correlated with February sea surface temperatures associated with similar ocean conditions that eventually lead to increased May–June krill densities on which the nestlings are fed [*Ainley et al.*, 1995; *Schroeder et al.*, 2009; *Black et al.*, 2011]. When juvenile salmon migrate from San Francisco Bay to the Gulf of the Farallones in May–June they feed on krill and, if not present in sufficient densities, significant mortality occurs [*Wells et al.*, 2012; *Woodson et al.*, 2013]. Finally, winter conditions may also determine transport of rockfish onto the shelf in spring where the rockfish rely on krill, and predators rely on the rockfish [*Reilly et al.*, 1992; *Wells et al.*, 2008; *Ralston et al.*, 2013].

To be robust and informative, marine ecosystem models and assessments require parameterized biophysical relationships that rely on realistic water column characteristics at appropriate spatial and temporal scales. Because survey costs can be prohibitive, alternative data sources such as output from the data-assimilative ROMS reanalysis become increasingly important, particularly in providing informed estimates for variables at fine spatiotemporal resolution. High-resolution model output, such as that presented here, can be useful for fitting habitat models and resolving temporally lagged functional relationships between species and ocean conditions at appropriate scales [*Hobday et al.*, 2011; *Huff et al.*, 2012; *Song et al.*, 2012], but continued model evaluation is critical to ensure results are reliable [*Santora et al.*, 2013].

References

Ainley, D. G., W. J. Sydeman, and J. Norton (1995), Upper trophic level predators indicate interannual negative and positive anomalies in the California Current food web, *Mar. Ecol. Prog. Ser.*, *118*(1–3), 69–79.

Black, B. A., I. D. Schroeder, W. J. Sydeman, S. J. Bograd, B. K. Wells, and F. B. Schwing (2011), Winter and summer upwelling modes and their biological importance in the California Current Ecosystem, *Global Change Biology*, *17*(8), 2536–2545.

Bograd, S. J., I. Schroeder, N. Sarkar, X. M. Qiu, W. J. Sydeman, and F. B. Schwing (2009), Phenology of coastal upwelling in the California Current, *Geophys. Res. Lett.*, *36*, L01602, doi:10.1029/2008GL035933.

Chelton, D. B., P. A. Bernal, and J. A. McGowan (1982), Large-scale interanual physical and biological interaction in the California Current, *J. Mar. Res.*, *40*, 1095–1123.

Collins, C. A., J. T. Pennington, C. G. Castro, T. A. Rago, and F. P. Chavez (2003), The California Current system off Monterey, California: Physical and biological coupling, *Deep Sea Res., Part II*, *50*(14–16), 2389–2404.

Croll, D. A., B. Marinovic, S. Benson, F. P. Chavez, N. Black, R. Ternullo, and B. R. Tershy (2005), From wind to whales: Trophic links in a coastal upwelling system, *Mar. Ecol. Prog. Ser.*, *289*, 117–130.

Dorman, J. G., S. M. Bollens, and A. M. Slaughter (2005), Population biology of euphausiids off northern California and effects of short time-scale wind events on *Euphausia pacifica*, *Mar. Ecol. Prog. Ser.*, *288*, 183–198.

Dorman, J. G., T. M. Powell, W. J. Sydeman, and S. J. Bograd (2011), Advection and starvation cause krill (*Euphausia pacifica*) decreases in 2005 Northern California coastal populations: Implications from a model study, *Geophys. Res. Lett.*, *38*, L04605, doi:10.1029/2010GL046245.

Feinberg, L. R., and W. T. Peterson (2003), Variability in duration and intensity of euphausiid spawning off central Oregon, 1996–2001, *Prog. Oceanogr.*, *57*(3–4), 363–379.

Fiechter, J., G. Broquet, A. M. Moore, and H. G. Arango (2011), A data assimilative, coupled physical–biological model for the Coastal Gulf of Alaska, *Dyn. Atmos. Oceans*, *52*(1–2), 95–118.

Field, J. C., A. D. MacCall, R. W. Bradley, and W. J. Sydeman (2010), Estimating the impacts of fishing on dependent predators: A case study in the California Current, *Ecol. Appl.*, *20*(8), 2223–2236.

Graham, W. W., and J. L. Largier (1997), Upwelling shadows as nearhsore retention sites: The example of northern Monterey Bay, *Cont. Shelf Res.*, *17*(5), 509–532.

Hobday, A. J., J. R. Hartog, C. M. Spillman, and O. Alves (2011), Seasonal forecasting of tuna habitat for dynamic spatial management, *Can. J. Fish. Aquat. Sci.*, *68*(5), 898–911.

Houde, E. D. (2008), Emerging from Hjort's shadow, *J. Northw. Atl. Fish. Sci.*, *41*, 53–70.

Huff, D. D., S. T. Lindley, B. K. Wells, and F. Chai (2012), Green sturgeon distribution in the Pacific Ocean estimated from modeled oceanographic features and migration behavior, *PLoS One*, *7*(9), e45852, doi:10.1371/journal.pone.0045852.

Ingleby, B., and M. Huddleston (2007), Quality control of ocean temperature and salinity profiles – historical and real-time data, *J. Mar. Syst.*, *65*, 158–175.

Ladd, C., and P. J. Stabeno (2012), Stratification on the Eastern Bering Sea shelf revisited, *Deep Sea Res., Part II*, *65–70*, 72–83.

Largier, J. L., et al. (2006), WEST: A northern California study of the role of wind-driven transport in the productivity of coastal plankton communities, *Deep Sea Res., Part II*, *53*(25–26), 2833–2849.

Lynn, R. J., S. J. Bograd, T. K. Chereskin, and A. Huyer (2003), Seasonal renewal of the California Current: The spring transition off California, *J. Geophys. Res.*, *108*(C8), 3279, doi:10.1029/2003JC001787.

Moore, A. M., H. G. Arango, G. Broquet, C. Edwards, M. Veneziani, B. Powell, D. Foley, J. D. Doyle, D. Costa, and P. Robinson (2011), The Regional Ocean Modeling System (ROMS) 4-dimensional variational data assimilation systems Part II - Performance and application to the California Current System, *Prog. Oceanogr.*, *91*(1), 50–73.

Palacios, D. M., E. L. Hazen, I. D. Schroeder, and S. J. Bograd (2013), Modeling the temperature-nitrate relationship in the coastal upwelling domain of the California Current, *J. Geophys. Res. Oceans*, *118*, 3223–3239, doi:10.1002/jgrc.20216.

Petersen, C. H., P. T. Drake, C. A. Edwards, and S. Ralston (2010), A numerical study of inferred rockfish (*Sebastes* spp.) larval dispersal along the central California coast, *Fish. Oceanogr.*, *19*(1), 21–41.

Ralston, S., K. M. Sakuma, and J. C. Field (2013), Interannual variation in pelagic juvenile rockfish (*Sebastes* spp.) abundance – going with the flow, *Fish. Oceanogr.*, *22*(4), 288–308.

Reilly, C. A., T. W. Echeverria, and S. V. Ralston (1992), Interannual variation and overlap in the diets of pelagic juvenile rockfish (Genus: *Sebastes*) off central California, *Fish. Bull.*, *90*, 505–515.

Santora, J. A., J. C. Field, I. D. Schroeder, K. M. Sakuma, B. K. Wells, and W. J. Sydeman (2012), Spatial ecology of krill, micronekton and top predators in the central California Current: Implications for defining ecologically important areas, *Prog. Oceanogr.*, *106*, 154–174.

Santora, J. A., W. J. Sydeman, M. Messie, F. Chai, Y. Chao, S. A. Thompson, B. K. Wells, and F. P. Chavez (2013), Triple check: Observations verify structural realism of an ocean ecosystem model, *Geophys. Res. Lett.*, *40*, 541–546, doi:10.1002/grl.50312.

Santora, J. A., I. D. Schroeder, J. C. Field, B. K. Wells, and W. J. Sydeman (2014), Spatio-temporal dynamics of ocean conditions and forage taxa reveals regional structuring of seabird-prey relationships, *Ecol. Appl.*, doi:10.1890/13-1605.1.

Schroeder, I. D., W. J. Sydeman, N. Sarkar, S. A. Thompson, S. J. Bograd, and F. B. Schwing (2009), Winter pre-conditioning of seabird phenology in the California Current, *Mar. Ecol. Prog. Ser.*, *393*, 211–223.

Schroeder, I. D., B. A. Black, W. J. Sydeman, S. J. Bograd, E. L. Hazen, J. A. Santora, and B. K. Wells (2013), The North Pacific High and wintertime pre-conditioning of California Current productivity, *Geophys. Res. Lett.*, *40*, 541–546, doi:10.1002/grl.50100.

Shchepetkin, A. F., and J. C. McWilliams (2005), The regional oceanic modeling system (ROMS): A split-explicit, free-surface, topography-following-coordinate oceanic model, *Ocean Model.*, *9*, 347–404.

Song, H., A. J. Miller, S. McClatchie, E. D. Weber, K. M. Nieto, and D. M. Checkley (2012), Application of a data-assimilation model to variability of Pacific sardine spawning and survivor habitats with ENSO in the California Current System, *J. Geophys. Res.*, *117*, C03009, doi:10.1029/2011JC007302.

Steger, J. M., F. B. Schwing, C. A. Collins, L. K. Rosenfeld, N. Garfield, and E. Gezgin (2000), The circulation and water masses in the Gulf of the Farallones, *Deep Sea Res., Part II*, *47*(5–6), 907–946.

Taylor, K. E. (2001), Summarizing multiple aspects of model performance in a single diagram, *J. Geophys. Res.*, *106*(D7), 7183–7192, doi:10.1029/2000JD900719.

Thayer, J. A., J. C. Field, and W. J. Sydeman (2014), Changes in California Chinook salmon diet over the past 50 years: Relevance to the recent population crash, *Mar. Ecol. Prog. Ser.*, *498*, 249–261.

Veneziani, M., C. A. Edwards, J. D. Doyle, and D. Foley (2009), A central California coastal ocean modeling study: 1. Forward model and the influence of realistic versus climatological forcing, *J. Geophys. Res.*, *114*, C04015, doi:10.1029/2008JC004774.

Wells, B. K., J. C. Field, J. A. Thayer, C. B. Grimes, S. J. Bograd, W. J. Sydeman, F. B. Schwing, and R. Hewitt (2008), Untangling the relationships among climate, prey and top predators in an ocean ecosystem, *Mar. Ecol. Prog. Ser.*, *364*, 15–29.

Wells, B. K., J. A. Santora, J. C. Field, R. B. MacFarlane, B. B. Marinovic, and W. J. Sydeman (2012), Population dynamics of Chinook salmon *Oncorhynchus tshawytscha* relative to prey availability in the central California coastal region, *Mar. Ecol. Prog. Ser.*, *457*, 125–137.

Woodson, L. E., B. K. Wells, P. K. Weber, R. B. MacFarlane, G. E. Whitman, and R. C. Johnson (2013), Size, growth, and origin-dependent mortality of juvenile Chinook salmon *Oncorhynchus tshawytscha* during early ocean residence, *Mar. Ecol. Prog. Ser.*, *487*, 163–175.